



OPEN Three-dimensional organ segmentation-derived CT attenuation parameters for assessing hepatic steatosis in chronic hepatitis B patients

Jeongin Yoo¹, Ijin Joo^{1,2,3,5}✉, Sun Kyung Jeon¹, Junghoan Park¹ & Eun Ju Cho⁴

The utility of CT-derived parameters for hepatic steatosis assessment has primarily focused on non-alcoholic fatty liver disease. This study aimed to evaluate their applicability in chronic hepatitis B (CHB) through a retrospective analysis of 243 CHB patients. Using deep-learning-based 3D organ segmentation on abdominal CT scans at 100 kVp, the mean volumetric CT attenuation of the liver and spleen was automatically measured on pre-contrast (liver (L)_pre and spleen (S)_pre) and post-contrast (L_post and S_post) portal venous phase images. To identify mild, moderate, and severe steatosis (S1, S2, and S3 based on the controlled attenuation parameter), L_pre showed areas under the receiver operating characteristic curve (AUROCs) of 0.695, 0.779, and 0.795, significantly higher than L-S_pre (0.633, 0.691, and 0.732; P s = 0.02, 0.003, and 0.03). Post-contrast parameters demonstrated slightly lower AUROCs than their pre-contrast counterparts (P s = 0.15–0.81). Concomitant hepatic fibrosis influenced diagnostic performance, with CT parameters performing better in patients without severe fibrosis than those with (F3–4 on transient elastography), though statistical significance was only observed for L-S_post in severe steatosis (P = 0.037). In conclusion, CT attenuation-based parameters extracted through automated 3D analysis show promise as a tool for assessing hepatic steatosis in patients with CHB.

Keywords Hepatic steatosis, Chronic hepatitis B, 3D segmentation, Deep learning, Computed tomography

Chronic hepatitis B (CHB) is a major global health concern that causes severe liver-related complications¹. One growing concern among CHB patients, particularly in endemic regions, is concomitant hepatic steatosis, which is increasingly prevalent and affects approximately 30% of patients with CHB^{2,3}. Hepatic steatosis in these patients results from a combination of viral mechanisms and metabolic risk factors, with the latter playing a more significant role⁴. Furthermore, the increasing prevalence of metabolic syndromes and obesity has contributed to the growing coexistence of hepatic steatosis and CHB⁵. The clinical implications of hepatic steatosis in patients with CHB have been studied from various perspectives. It is associated with a higher rate of hepatitis B surface antigen seroclearance, which may reduce the risk of hepatocellular carcinoma (HCC)⁶. However, in these patients, the metabolic abnormalities associated with steatosis independently increase the risk of HCC, complicating the overall impact of steatosis⁶. While the presence of hepatic steatosis in patients with CHB is not directly associated with the severity of liver fibrosis⁷, it is correlated with worse metabolic profiles and a higher risk of cardiovascular disease⁸. Therefore, accurate assessment of steatosis in patients with CHB could be crucial for predicting patient prognosis and identifying high-risk groups.

B-mode ultrasound is the primary screening modality for the non-invasive assessment of hepatic steatosis; however, other modalities that provide quantitative measurements, such as transient elastography (TE) with controlled attenuation parameter (CAP), magnetic resonance imaging proton density fat fraction (MRI-PDFF),

¹Department of Radiology, Seoul National University Hospital, Seoul, Korea. ²Department of Radiology, Seoul National University College of Medicine, Seoul, Korea. ³Institute of Radiation Medicine, Medical Research Center, Seoul National University, Seoul National University Hospital, Seoul, Korea. ⁴Department of Internal Medicine, Liver Research Institute, Seoul National University College of Medicine, Seoul, Korea. ⁵Department of Radiology, Seoul National University Hospital, Seoul National University College of Medicine, 101 Daehak-ro, Jongno-gu, Seoul 03080, Korea. ✉email: hijjin@gmail.com

and quantitative ultrasound, have gained attention, given their good diagnostic performance and high inter-observer reliability^{9,10}. In contrast, computed tomography (CT) is not typically preferred for evaluating hepatic steatosis owing to its reliance on ionizing radiation. However, its role as a standard imaging tool for various clinical conditions has led to the recognition of its potential for opportunistic screening¹¹. Hepatic steatosis assessment on CT has traditionally relied on 2D region-of-interest (ROI) measurements, while 3D automated volumetric analysis has been increasingly utilized in recent studies, both showing favorable diagnostic performance¹². Indeed, using deep-learning-based organ segmentation, CT-derived 3D parameters for hepatic steatosis can be automatically extracted from large-scale cohorts¹³, and recent studies have highlighted their utility^{14,15}.

Patients with CHB undergo regular HCC surveillance, primarily using ultrasonography. However, in settings where ultrasonography is not optimal, CT can be used as an alternative tool^{16,17}. Moreover, diagnostic CT is performed when suspicious lesions are found on ultrasonography or when other comorbidities need to be evaluated. Therefore, if CT, primarily performed for these purposes, is validated as a tool to assess concomitant hepatic steatosis, it would be useful in assessing and monitoring associated metabolic abnormalities in patients with CHB. Until now, most studies using CT to evaluate steatosis have focused on nonalcoholic fatty liver disease (NAFLD), which does not include steatosis associated with viral hepatitis in its definition¹⁸. However, data on patients with CHB concerning this aspect remain unavailable.

Therefore, we aimed to evaluate the use of CT attenuation-based parameters acquired from automated 3D organ segmentation to assess hepatic steatosis in patients with CHB.

Materials and methods

This retrospective study was approved by the institutional review board of Seoul National University Hospital (IRB No. H-2306-112-1439), which waived the requirement for informed consent due to its retrospective nature. The study was conducted in accordance with the Declaration of Helsinki.

Patients

Using a computerized search of the radiological database and electronic medical records at our institution, we identified patients with CHB who underwent liver CT scans and TE with CAP between January 2021 and December 2023 (Fig. 1). The inclusion criteria were as follows: (1) age ≥ 18 years; (2) liver CT scans performed at 100 kVp; CT attenuation values are affected by tube voltage; therefore, we selected one specific kVp setting for this study; and (3) a time interval of < 60 days between the CT scan and TE. The exclusion criteria were as follows: (1) definite focal liver lesions (> 1 cm) on CT scans; (2) a history of liver surgery or locoregional therapy; (3) undergoing splenectomy; and (4) technical failure of TE. The acquisition protocols for liver CT scans and TE with CAP are described in the Supplementary material.

CT attenuation measurement of the liver and spleen

Using an automated 3D organ segmentation algorithm, volumetric CT attenuation values for the liver and spleen were measured (Fig. 2). For each patient, measurements were obtained on pre- and post-contrast images. The portal venous phase was selected for postcontrast imaging because of its broad application in routine practice and hepatic steatosis research. Additionally, the conventional 2D ROI-based measurement method, which has been typically used in previous studies, was compared with the 3D approach. A detailed description of each measurement method is provided below.

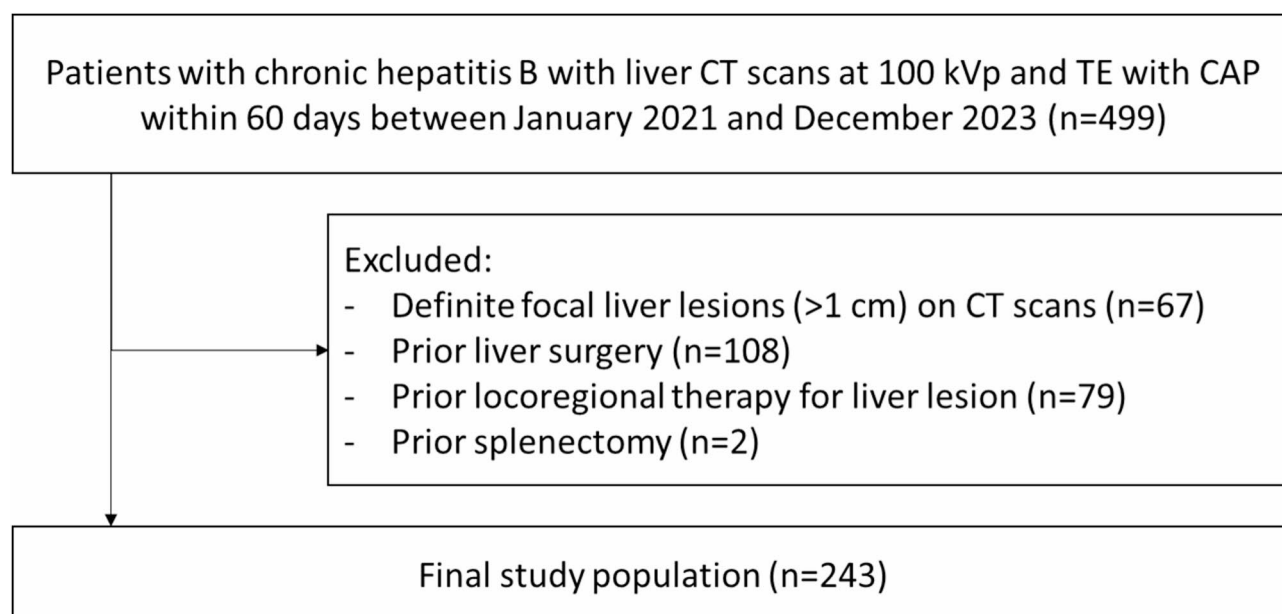


Fig. 1. Flowchart. TE = transient elastography, CAP = controlled attenuation parameter.

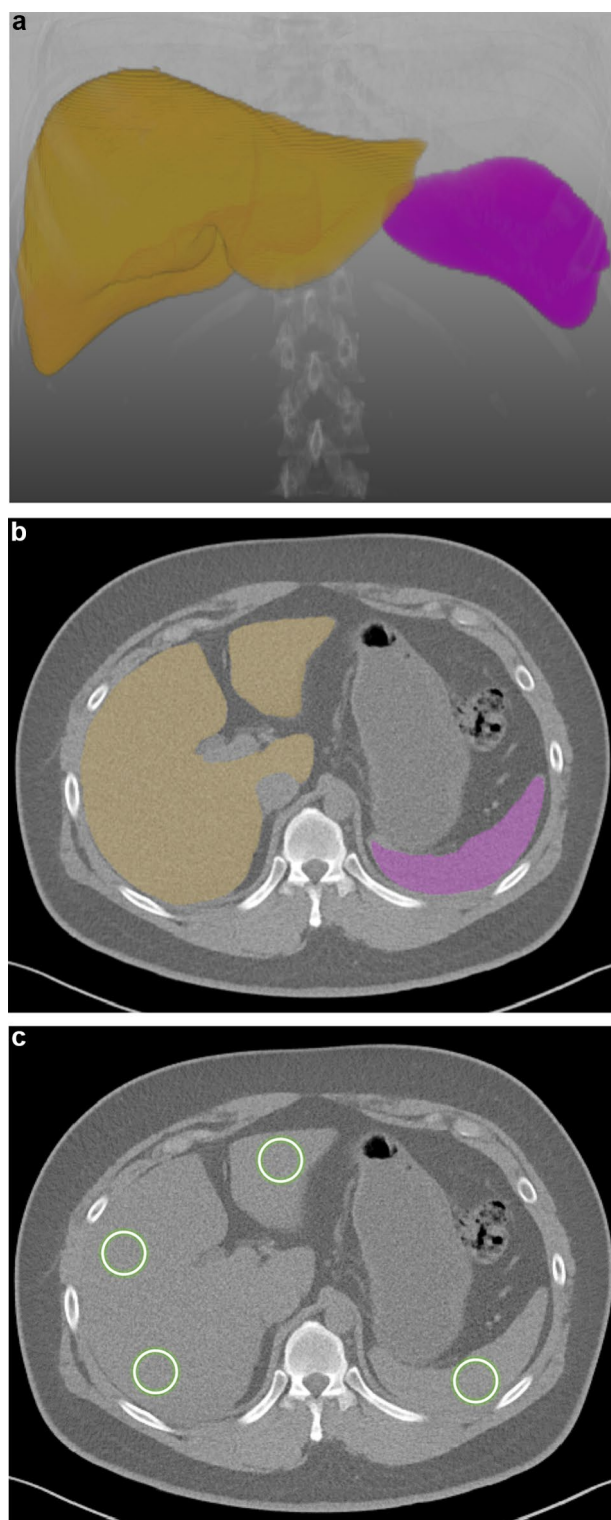


Fig. 2. Liver CT scan of a 35-year-old man with chronic hepatitis B and severe steatosis, with a controlled attenuation parameter value of 312. Fully automated 3D segmentation of the liver and spleen was performed on pre-contrast (a–c) and post-contrast images (d–f). Based on the 3D organ segmentation (a, d: 3D volume rendering images; b, e: axial images showing liver and spleen segmentation), the volumetric mean CT attenuation values were automatically measured as follows: $L_{pre} = 31.1$ HU, $S_{pre} = 39.1$ HU; $L_{post} = 116.4$ HU, $S_{post} = 143.2$ HU. Accordingly, $L-S_{pre} = -8.0$ HU and $L-S_{post} = -26.8$ HU, indicating severe steatosis. CT attenuation measurements using the 2D region-of-interest method on axial sections (c, f) were 35.6 HU and 42.2 HU for the liver and spleen on the pre-contrast image, and 115.8 HU and 154.5 HU on the post-contrast image. L = mean CT attenuation values of the liver; S = mean CT attenuation values of the spleen; $L-S = L$ minus S.

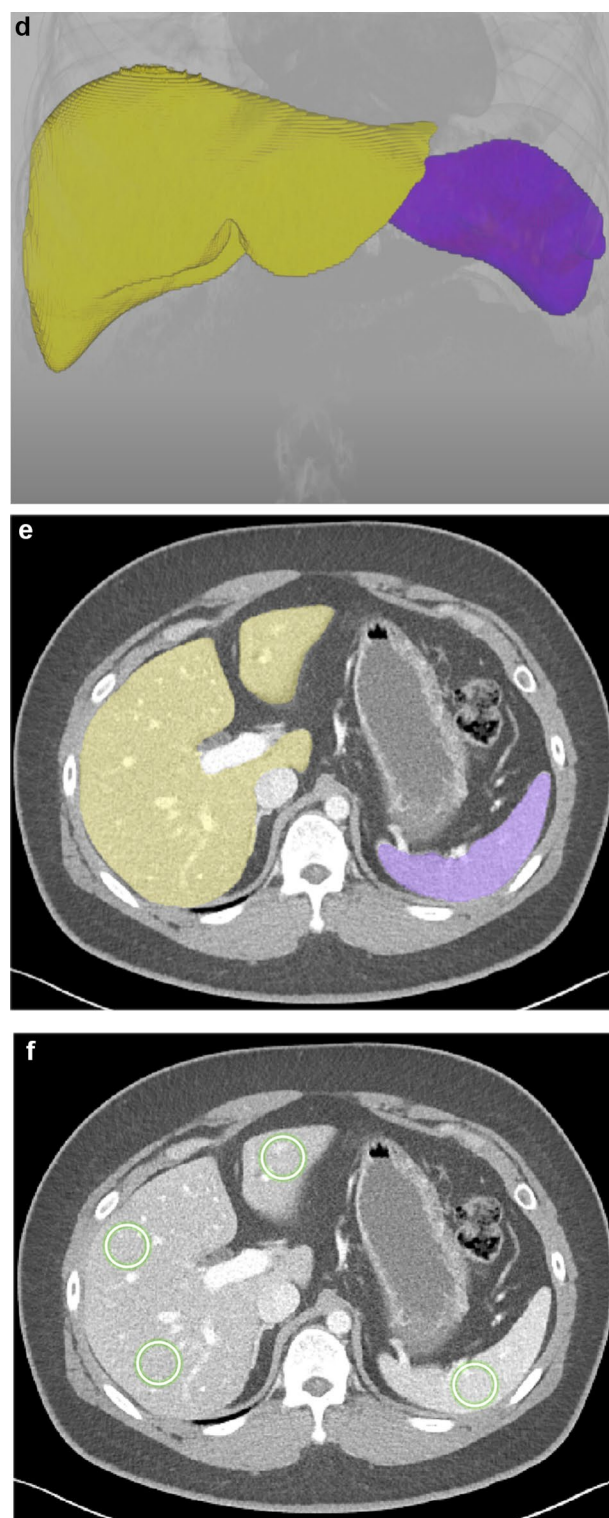


Figure 2. (continued)

Manual 2D ROI-based measurement

To measure CT attenuation of the liver and spleen using 2D ROIs (Fig. 2), a board-certified radiologist (BLINDED) placed three circular ROIs in the liver of each patient: one in the left lobe, one in the right anterior section, and one in the right posterior section. In addition, a single circular ROI was placed in the central portion of the spleen. This methodology was based on a previous study¹⁴. The ROIs were drawn using a picture archiving and communication system (INFINITT PACS M6; INFINITT Healthcare). Care was taken to ensure that the ROIs, measuring 250–300 mm², were placed in regions that avoided vessels, focal lesions, and other causes of

heterogeneity, including artifacts. Initially, the ROIs were drawn on the post-contrast images and transferred to the corresponding pre-contrast images to ensure consistent anatomical positioning across both sets of images. The average of the mean HU values of the three liver ROIs was calculated separately for the pre- and post-contrast images and denoted as L_pre and L_post, respectively. Similarly, the mean HU values of the spleen ROI were denoted as S_pre and S_post.

Volumetric measurement using a 3D multi-organ segmentation algorithm

A commercially available multi-organ segmentation program (DeepCatch v1.3.0, MEDICAL IP Co. Ltd.), developed based on the 3D nnU-Net algorithm, was used to obtain volumetric CT attenuation measurements for the liver and spleen from the CT Digital Imaging and Communications in Medicine (DICOM) files. This program automatically segmented the liver and spleen, generating a 3D mask representing these organs¹⁹, and then computed the volumetric mean of the CT attenuation values for the liver and spleen (L_pre and S_pre) on pre-contrast images and L_post and S_post on post-contrast images using all designated voxels from the respective images.

CT attenuation-based parameters for assessing hepatic steatosis

Following previous studies^{20,21}, L_pre and liver-minus-spleen [L-S]_pre on pre-contrast images and L_post and L-S_post on post-contrast images were examined as CT attenuation-based parameters for assessing hepatic steatosis.

Transient elastography with controlled attenuation parameters

Hepatic steatosis grades were determined based on CAP values, following the cutoff thresholds from a previous meta-analysis²²: <248 dB/m for S0 (no steatosis), 248–267 dB/m for S1 (mild steatosis), 268–279 dB/m for S2 (moderate steatosis), and ≥280 dB/m for S3 (severe steatosis). These CAP grades correspond to the pathological grades of hepatic steatosis: S0 with fatty changes in <5% of the hepatocytes, S1 in 5–33%, S2 in 34–66%, and S3 in >66%.²³ CAP has limitations, such as accuracy being influenced by factors like body mass index; however, it is often used as a standard reference for assessing hepatic steatosis in clinical and research settings, with reported areas under the receiver operating characteristic (ROC) curve (AUROC) of 0.96, 0.82 and 0.70 for S1, S2, and S3, respectively²⁴. Hepatic fibrosis grades were determined using liver stiffness measurement (LSM) values based on the cutoff thresholds suggested in a multicenter prospective study of patients with CHB²⁵: <7.2 kPa for F0 or F1 (no or mild fibrosis), ≥7.2 kPa and <8.1 kPa for F2 (significant fibrosis), ≥8.1 kPa and <11 kPa for F3 (severe fibrosis), and ≥11 kPa for F4 (cirrhosis).

Statistical analysis

All statistical analyses were performed using the IBM SPSS Statistics for Windows (version 29.0; IBM Corp) and MedCalc Statistical Software (version 18.9.1, MedCalc Software bvba). Statistical significance was set at $p < 0.05$.

The agreement between volumetric and manual ROI-based measurements of CT attenuation values of the liver and spleen was assessed using the intraclass correlation coefficient (ICC) and Bland–Altman analysis. According to the ICC estimates, values < 0.5, 0.5–0.75, 0.75–0.9, and > 0.90 indicated poor, moderate, good, and excellent agreements, respectively.

Volumetric CT attenuation-based parameters for hepatic steatosis (L_pre, L-S_pre, L_post, and L-S_post) were evaluated to detect mild, moderate, and severe hepatic steatosis (S1, S2, and S3, respectively, based on CAP values) using ROC curve analysis. Additionally, the diagnostic performance of volumetric parameters was compared with that of 2D ROI-based measurements to assess differences between the two approaches. The AUROCs were used to assess diagnostic performance and were compared between the CT parameters using z-statistics. Cutoff values of CT parameters for identifying mild, moderate, and severe steatosis were determined to maximize the Youden index, achieving >80% sensitivity, and >80% specificity, respectively. The corresponding sensitivity and specificity values were then computed. Additionally, using z-statistics, the effect of hepatic fibrosis by comparing the AUROCs of patients with severe hepatic fibrosis (F3 to F4 based on LSM values) with those without severe fibrosis (F0 to F2).

Results

Patient characteristics

The final study population comprised 243 patients with CHB (119 men; mean age, 57.9 years). Based on the CAP values, 71 (29.2%) had hepatic steatosis (S1 to S3). According to the LSM values, 70 (28.8%) patients had severe fibrosis (F3 or F4), whereas the remaining 173 did not. Table 1 shows the detailed patient characteristics.

Agreements between volumetric and 2D ROI-based measurements

For the liver, volumetric measurements of L_pre and L_post showed excellent agreements with their ROI-based counterparts, with ICC values of 0.947 (95% confidence interval [CI]: 0.932–0.959) and 0.949 (95% CI: 0.934–0.960), and mean differences of -3.1 HU and -0.5 HU, respectively (Supplementary Fig. 1).

However, for the spleen, the volumetric measurements of S_pre and S_post demonstrated good agreements with their ROI-based counterparts, with ICC values of 0.840 (95% CI: 0.794–0.876) and 0.894 (95% CI: 0.864–0.918), and mean differences of -5.1 HU and -8.0 HU, respectively (Supplementary Fig. 1).

Diagnostic performance of volumetric CT parameters for hepatic steatosis

Of pre-contrast CT parameters, L_pre showed AUROCs of 0.695, 0.779, and 0.795, for identifying mild, moderate, and severe steatosis, respectively, which were significantly higher than those of L-S_pre (0.633, 0.691, and 0.732; P s = 0.02, 0.003, and 0.03, respectively) (Table 2) (Supplementary Fig. 2).

Characteristics (<i>n</i> =273)	Value
Age (y), mean \pm SD (range)	57.9 \pm 10.7 (30–86)
Sex	
Male	119 (49.0)
Female	124 (51.0)
Liver stiffness measurements (kPa)	
Mean \pm SD (range)	8.2 \pm 7.5 (3.2–39.5)
Fibrosis grades	
F0 or F1 (< 7.2 kPa)	162 (66.7)
F2 (\geq 7.2 kPa and < 8.1 kPa)	11 (4.5)
F3 (\geq 8.1 kPa and < 11 kPa)	33 (13.6)
F4 (\geq 11 kPa)	37 (15.2)
Controlled attenuation parameter measurements (dB/m)	
Mean \pm SD (range)	225 \pm 52 (103–374)
Steatosis grades	
S0 (< 248 dB/m)	172 (70.8)
S1 (\geq 248 dB/m and < 268 dB/m)	28 (11.5)
S2 (\geq 268 dB/m and < 280 dB/m)	10 (4.1)
S3 (\geq 280 dB/m)	33 (13.6)

Table 1. Characteristics of the study population. Note. – Unless otherwise specified, data are number of patients with percentages in parentheses. SD, standard deviation.

Volumetric CT parameters	Hepatic steatosis grades		
	At least mild	At least moderate	Severe
AUROC (95% CI)			
L_pre	0.695 (0.633–0.752)	0.779 (0.722–0.830)	0.795 (0.738–0.844)
L-S_pre	0.633 (0.569–0.694)	0.691 (0.629–0.749)	0.732 (0.672–0.787)
L_post	0.681 (0.619–0.739)	0.712 (0.651–0.768)	0.744 (0.685–0.798)
L-S_post	0.623 (0.559–0.684)	0.675 (0.612–0.733)	0.698 (0.636–0.755)
P values*			
L_pre vs. L-S_pre	0.02	0.003	0.03
L_post vs. L-S_post	0.20	0.42	0.29
L_pre vs. L_post	0.74	0.15	0.31
L-S_pre vs. L-S_post	0.81	0.74	0.54

Table 2. Diagnostic performances of CT attenuation-based parameters for assessing hepatic steatosis. Note. – AUROC, area under the receiver operating characteristic curve; CI, confidence interval; L_pre and L_post refer to the mean liver HU on pre- and post-contrast CT images, respectively; L-S_pre and L-S_post refer to the difference in mean HU between the liver and spleen on pre- and post-contrast CT images, respectively.

*Calculated using z-statistics.

Of post-contrast CT parameters, L_post showed slightly higher AUROCs compared with those of L-S_post for detecting mild (0.681 vs. 0.623), moderate (0.712 vs. 0.675), and severe steatosis (0.744 vs. 0.698). However, these differences were not statistically significant ($P=0.20$, 0.42, and 0.29, respectively) (Table 2) (Supplementary Fig. 2).

For all grades of steatosis, pre-contrast CT parameters showed slightly higher AUROCs than post-contrast counterparts; however, the differences were not statistically significant ($P_s=0.15$ –0.81) (Table 2).

Cutoff values of each CT parameters for mild, moderate, and severe steatosis are described in Supplementary Table 1.

Comparison with 2D ROI-based parameters

For the assessment of all degrees of hepatic steatosis, the AUROCs of volumetric parameters did not differ significantly from those of 2D ROI-based measurements ($P_s=0.11$ –0.90) (Supplementary Table 2).

Effect of hepatic fibrosis on diagnostic performance of CT parameters for hepatic steatosis

In the comparative analysis between patients with and without severe fibrosis, all assessed CT parameters consistently showed lower AUROCs in patients with severe fibrosis than in those without severe fibrosis (Table 3). These differences were not statistically significant across all parameters for detecting mild ($P_s=0.15$ –

Hepatic steatosis grades	CT parameters	AUROC (95% CI)		P-value*
		Patients with severe fibrosis (n = 70)	Patients without severe fibrosis (n = 173)	
Mild	L_pre	0.645 (0.521–0.756)	0.698 (0.623–0.765)	0.56
	L-S_pre	0.568 (0.444–0.686)	0.634 (0.557–0.706)	0.48
	L_post	0.623 (0.499–0.736)	0.694 (0.620–0.762)	0.40
	L-S_post	0.516 (0.394–0.638)	0.642 (0.566–0.713)	0.15
Moderate	L_pre	0.676 (0.554–0.783)	0.804 (0.737–0.861)	0.22
	L-S_pre	0.616 (0.492–0.730)	0.707 (0.633–0.773)	0.43
	L_post	0.621 (0.497–0.734)	0.744 (0.673–0.808)	0.19
	L-S_post	0.564 (0.440–0.682)	0.706 (0.633–0.773)	0.15
Severe	L_pre	0.659 (0.536–0.769)	0.843 (0.781–0.894)	0.13
	L-S_pre	0.687 (0.565–0.793)	0.742 (0.670–0.806)	0.66
	L_post	0.706 (0.585–0.809)	0.755 (0.684–0.817)	0.58
	L-S_post	0.525 (0.402–0.646)	0.765 (0.695–0.826)	0.037

Table 3. Comparison of diagnostic performance of CT attenuation-based parameters for assessing hepatic steatosis between patients with and without severe fibrosis. Note. – AUROC, area under the receiver operating characteristic curve; CI, confidence interval; L_pre and L_post refer to the mean liver HU on pre- and post-contrast CT images, respectively; L-S_pre and L-S_post refer to the difference in mean HU between the liver and spleen on pre- and post-contrast CT images, respectively. *Calculated using z-statistics.

0.56) or moderate steatosis (Ps = 0.15–0.43) (Table 3). However, a statistically significant difference was observed in the detection of severe steatosis using L-S_post, with patients with severe fibrosis demonstrating significantly lower AUROCs than those without severe fibrosis (0.53 vs. 0.77, $P = 0.037$), although no significant differences were found for L_pre, L-S_pre, or L_post (Table 3).

Discussion

In our study, we demonstrated that volumetric CT attenuation-based parameters acquired using a fully automated 3D segmentation tool exhibited promising potential for detecting and grading hepatic steatosis in patients with CHB, though their diagnostic performance to be modest. Our results suggest that in patients with CHB, where CT scans are frequently used for surveillance or diagnostic purposes, CT attenuation-based parameters derived from 3D segmentation could be a valuable tool for evaluating hepatic steatosis. This result can be explained by the underlying phenomenon in fatty livers, where the liver’s CT attenuation value decreases, and enhancement is reduced²⁶, which is consistent with previous studies demonstrating the applicability of these changes as quantitative parameters^{13,21}. Our study is novel because, whereas other analyses have primarily been applied within the context of conventional NAFLD, our results support extending the use of 3D CT analysis for assessing steatosis to a broader range of conditions, including CHB.

In our study, comparing liver and spleen CT attenuation based on different measurement methods, volumetric CT attenuation parameters showed good-to-excellent agreement with ROI-based parameters, as indicated by the high ICC values. However, volumetric measurements were slightly lower than ROI-based measurements, which are consistent with previous studies¹⁴. This discrepancy may be owing to manual ROI placement, which deliberately selects visually homogeneous areas, whereas volumetric measurements encompass the entire organ volume. These results suggest that the 2D ROI-based and 3D volumetric measurements have systematic differences and are not fully interchangeable. Therefore, the interpretation and cutoff values should consider this difference.

For volumetric pre-contrast parameters, our results demonstrated higher AUCs for L_pre than for L-S_pre, despite the latter being designed to improve reliability by using the spleen as an internal reference to detect any degree of hepatic steatosis. Notably, both parameters have been widely used as indicators of steatosis in various studies²⁷, and studies comparing them have shown similar efficacy^{14,28}. However, in our study, L_pre was superior, which may be attributed to the differences in the study populations from previous studies: patients with CHB patients versus healthy participants. In patients with CHB, the accompanying portal hypertension can lead to splenomegaly, which could affect the CT attenuation value of the spleen. Our study found a significant positive correlation between splenic volume and S_pre ($r = 0.297$, $P < 0.001$) (data not shown). Therefore, using spleen HU for normalization might have reduced the diagnostic performance compared with using liver HU alone, especially in settings where such factors may impact spleen attenuation. Regarding post-contrast CT parameters, L-S_post also showed slightly lower AUCs than L_post. This finding is consistent with that of a recent study in healthy participants²⁶ which demonstrated the superiority of L_post over L-S_post in detecting moderate steatosis using CT. Our results suggest that evaluating steatosis in patients with CHB might be more appropriate using liver attenuation alone for pre- and post-contrast CT imaging.

Our study results demonstrated the reduced diagnostic performance of CT parameters in patients with severe fibrosis; however, statistical significance was found only when using L-S_post for detecting severe steatosis, suggesting that fibrosis may influence CT attenuation values. This observation is consistent with previous studies, indicating that liver CT attenuation increases with hepatic fibrosis²⁹. CT attenuation typically correlates with steatosis; however, the presence of fibrosis may reduce its accuracy in assessing steatosis. These findings

emphasize the need to consider the fibrosis grade when using CT attenuation to evaluate steatosis in patients with chronic liver disease or cirrhosis. Future research should explore these interactions more thoroughly using multiparametric MRI assessments. Additionally, as CT radiomics features have been reported to be associated with fibrosis^{30,31}, a comprehensive analysis of CT quantitative parameters could be beneficial. This approach could help identify suitable patient groups for hepatic steatosis evaluation using CT, even in the presence of underlying liver disease, or enable independent prediction of steatosis through multivariate analysis.

This study has some limitations. First, a potential selection bias is unavoidable owing to its retrospective nature. Our study population, which underwent liver CT, might have included patients at a high risk of HCC occurrence or those with poor ultrasound visibility, considering that most patients with CHB patients undergo surveillance ultrasonography rather than CT. Therefore, further prospective investigations are warranted to confirm the results of our study in the general population with CHB. Second, the CAP was used as a reference standard for hepatic steatosis. TE with CAP is widely used in patients with CHB, allowing the simultaneous evaluation of fibrosis and steatosis; however, the cutoff value of CAP is not well standardized and varies across studies⁹. Moreover, although CAP performs well in diagnosing mild steatosis, its accuracy tends to decline when diagnosing moderate or higher grades of steatosis²⁴. Therefore, further evaluation using a well-established standard reference for hepatic steatosis, such as MRI-PDFF, would be necessary. Finally, our study included CT scans obtained at 100 kVp, which was selected considering that CT attenuation values are influenced by kVp settings. However, various kVp settings are clinically utilized; therefore, additional research is required to establish applicable cutoff values across different scan settings to ensure a broader generalization.

In conclusion, CT attenuation-based parameters acquired through automated 3D organ segmentation show promise as a tool for assessing hepatic steatosis in patients with CHB. ,

Data availability

The data used to support the findings of this study are available from the corresponding author on reasonable request.

Received: 7 January 2025; Accepted: 25 March 2025

Published online: 06 April 2025

References

- Lim, J. K. et al. Prevalence of chronic hepatitis B virus infection in the united States. *Am. J. Gastroenterol.* **115**, 1429–1438. <https://doi.org/10.14309/ajg.0000000000000651> (2020).
- Jiang, D. et al. Concurrence and impact of hepatic steatosis on chronic hepatitis B patients: a systematic review and meta-analysis. *Ann. Transl. Med.* **9**, 1718. <https://doi.org/10.21037/atm-21-3052> (2021).
- Zheng, Q. et al. Systematic review with meta-analysis: prevalence of hepatic steatosis, fibrosis and associated factors in chronic hepatitis B. *Aliment. Pharmacol. Ther.* **54**, 1100–1109. <https://doi.org/10.1111/apt.16595> (2021).
- Machado, M. V., Oliveira, A. G. & Cortez-Pinto, H. Hepatic steatosis in hepatitis B virus infected patients: meta-analysis of risk factors and comparison with hepatitis C infected patients. *J. Gastroenterol. Hepatol.* **26**, 1361–1367. <https://doi.org/10.1111/j.1440-1746.2011.06801.x> (2011).
- Bondini, S. et al. Impact of non-alcoholic fatty liver disease on chronic hepatitis B. *Liver Int.* **27**, 607–611. <https://doi.org/10.1111/j.1478-3231.2007.01482.x> (2007).
- Yu, M. W. et al. Metabolic-Associated fatty liver disease, hepatitis B surface antigen seroclearance, and Long-Term risk of hepatocellular carcinoma in chronic hepatitis B. *Cancers (Basel)*. **14**. <https://doi.org/10.3390/cancers14236012> (2022).
- Choi, H. S. J. et al. Nonalcoholic steatohepatitis is associated with Liver-Related outcomes and All-Cause mortality in chronic hepatitis B. *Hepatology* **71**, 539–548. <https://doi.org/10.1002/hep.30857> (2020).
- Leow, Y. W. et al. Hepatic steatosis and metabolic risk factors among patients with chronic hepatitis B: the multicentre, prospective CAP-Asia study. *J. Viral Hepat.* **30**, 319–326. <https://doi.org/10.1111/jvh.13796> (2023).
- Park, J., Lee, J. M., Lee, G., Jeon, S. K. & Joo, I. Quantitative evaluation of hepatic steatosis using advanced imaging techniques: focusing on new quantitative ultrasound techniques. *Korean J. Radiol.* **23**, 13–29. <https://doi.org/10.3348/kjr.2021.0112> (2022).
- Dag, N., Igci, G., Yagin, F. H., Hanci, Muhammed, S. & Kutlu, R. Interobserver Reproducibility of Ultrasound Attenuation Imaging Technology in Liver Fat Quantification. *J. Clin. Ultrasound* n/a. <https://doi.org/10.1002/jcu.23877>
- Pickhardt, P. J. Value-added opportunistic CT screening: state of the Art. *Radiology* **303**, 241–254. <https://doi.org/10.1148/radiol.211561> (2022).
- Haghshomar, M. et al. Diagnostic accuracy of CT for the detection of hepatic steatosis: A systematic review and Meta-Analysis. *Radiology* **313**, e241171. <https://doi.org/10.1148/radiol.241171> (2024).
- Graffy, P. M., Sandfort, V., Summers, R. M. & Pickhardt, P. J. Automated liver fat quantification at nonenhanced abdominal CT for Population-based steatosis assessment. *Radiology* **293**, 334–342. <https://doi.org/10.1148/radiol.2019190512> (2019).
- Yoo, J., Joo, I., Jeon, S. K., Park, J. & Yoon, S. H. Utilizing fully-automated 3D organ segmentation for hepatic steatosis assessment with CT attenuation-based parameters. *Eur. Radiol.* 1–9. <https://doi.org/10.1007/s00330-024-10660-4> (2024).
- Pickhardt, P. J. et al. Liver steatosis categorization on contrast-enhanced CT using a fully automated deep learning volumetric segmentation tool: evaluation in 1204 healthy adults using unenhanced CT as a reference standard. *Am. J. Roentgenol.* **217**, 359–367. <https://doi.org/10.2214/AJR.20.24415> (2021).
- American College of Radiology Committee on LI-RADS. LI-RADS® Ultrasound Surveillance v2024 Core (2024). <https://edge.sitecorecloud.io/americancoldf5f-acrorgf92a-productioncb02-3650/media/ACR/Files/RADS/LI-RADS/LI-RADS-US-Surveillance-v2024-Core.pdf>
- Korean Liver Cancer Association. KLCA-NCC Korea practice guidelines for the management of hepatocellular carcinoma. *Korean Journal of Radiology* **23**, 1126. (2022). <https://doi.org/10.3348/kjr.2022.0822>.
- Eslam, M. et al. A new definition for metabolic dysfunction-associated fatty liver disease: an international expert consensus statement. *J. Hepatol.* **73**, 202–209. <https://doi.org/10.1016/j.jhep.2020.03.039> (2020).
- Jeon, S. K. et al. Fully-automated multi-organ segmentation tool applicable to both non-contrast and post-contrast abdominal CT: deep learning algorithm developed using dual-energy CT images. *Sci. Rep.* **14**, 4378. <https://doi.org/10.1038/s41598-024-55137-y> (2024).
- Byun, J. et al. CT indices for the diagnosis of hepatic steatosis using non-enhanced CT images: development and validation of diagnostic cut-off values in a large cohort with pathological reference standard. *Eur. Radiol.* **29**, 4427–4435. <https://doi.org/10.1007/s00330-018-5905-1> (2019).

21. Guo, Z. et al. Liver fat content measurement with quantitative CT validated against MRI proton density fat fraction: A prospective study of 400 healthy volunteers. *Radiology* **294**, 89–97. <https://doi.org/10.1148/radiol.2019190467> (2020).
22. Karlas, T. et al. Individual patient data meta-analysis of controlled Attenuation parameter (CAP) technology for assessing steatosis. *J. Hepatol.* **66**, 1022–1030. <https://doi.org/10.1016/j.jhep.2016.12.022> (2017).
23. Kleiner, D. E. et al. Design and validation of a histological scoring system for nonalcoholic fatty liver disease. *Hepatology* **41**, 1313–1321. <https://doi.org/10.1002/hep.20701> (2005).
24. Pu, K. et al. Diagnostic accuracy of controlled Attenuation parameter (CAP) as a non-invasive test for steatosis in suspected non-alcoholic fatty liver disease: a systematic review and meta-analysis. *BMC Gastroenterol.* **19**, 1–11. <https://doi.org/10.1186/s12876-019-0961-9> (2019).
25. Marcellin, P. et al. Non-invasive assessment of liver fibrosis by stiffness measurement in patients with chronic hepatitis B. *Liver Int.* **29**, 242–247. <https://doi.org/10.1111/j.1478-3231.2008.01802.x> (2009).
26. Pickhardt, P. J., Blake, G. M., Moeller, A., Garrett, J. W. & Summers, R. M. Post-contrast CT liver Attenuation alone is superior to the liver–spleen difference for identifying moderate hepatic steatosis. *Eur. Radiol.* 1–12. <https://doi.org/10.1007/s00330-024-10816-2> (2024).
27. Starekova, J., Hernando, D., Pickhardt, P. J. & Reeder, S. B. Quantification of liver fat content with CT and MRI: state of the Art. *Radiology* **301**, 250–262. <https://doi.org/10.1148/radiol.2021204288> (2021).
28. Park, S. H. et al. Macrovesicular hepatic steatosis in living liver donors: use of CT for quantitative and qualitative assessment. *Radiology* **239**, 105–112. <https://doi.org/10.1148/radiol.2391050361> (2006).
29. Lubner, M. G., Malecki, K., Kloke, J., Ganeshan, B. & Pickhardt, P. J. Texture analysis of the liver at MDCT for assessing hepatic fibrosis. *Abdom. Radiol. (NY)*. **42**, 2069–2078. <https://doi.org/10.1007/s00261-017-1096-5> (2017).
30. Wang, J. et al. Radiomics analysis of contrast-enhanced CT for staging liver fibrosis: an update for image biomarker. *Hepatol. Int.* **16**, 627–639. <https://doi.org/10.1007/s12072-022-10326-7> (2022).
31. Wang, X. M. & Zhang, X. J. Role of radiomics in staging liver fibrosis: a meta-analysis. *BMC Med. Imaging*. **24**, 87. <https://doi.org/10.1186/s12880-024-01272-x> (2024).

Author contributions

Conceptualization: I.J.; Data curation: J.Y.; Formal analysis: J.Y.; Methodology: all authors; Writing—original draft: J.Y.; Writing—review and editing: all authors.

Funding

This work was supported by the New Faculty Startup Fund from Seoul National University; National Research Foundation of Korea (NRF) grant funded by the Korean government (MSIT) (RS-2023-00253896).

Statements and declarations

Competing interests

The authors have no disclosures to declare.

Additional information

Supplementary Information The online version contains supplementary material available at <https://doi.org/10.1038/s41598-025-96053-z>.

Correspondence and requests for materials should be addressed to I.J.

Reprints and permissions information is available at www.nature.com/reprints.

Publisher's note Springer Nature remains neutral with regard to jurisdictional claims in published maps and institutional affiliations.

Open Access This article is licensed under a Creative Commons Attribution-NonCommercial-NoDerivatives 4.0 International License, which permits any non-commercial use, sharing, distribution and reproduction in any medium or format, as long as you give appropriate credit to the original author(s) and the source, provide a link to the Creative Commons licence, and indicate if you modified the licensed material. You do not have permission under this licence to share adapted material derived from this article or parts of it. The images or other third party material in this article are included in the article's Creative Commons licence, unless indicated otherwise in a credit line to the material. If material is not included in the article's Creative Commons licence and your intended use is not permitted by statutory regulation or exceeds the permitted use, you will need to obtain permission directly from the copyright holder. To view a copy of this licence, visit <http://creativecommons.org/licenses/by-nc-nd/4.0/>.

© The Author(s) 2025